J Mater Sci (2010) 45:5534–5542
DOI 10.1007/s10853-010-4613-2

Wet hydrogen sulfide cracking of steel monitoring by acoustic emission: discrimination of AE sources

Véronique Smanio · Marion Fregonese · Jean Kittel · Thierry Cassagne · François Ropital · Bernard Normand

Received: 21 December 2009 / Accepted: 11 May 2010 / Published online: 22 May 2010

Abstract In the petroleum industry, it is known that equipments which operate in wet hydrogen sulfide (H_2S) media can be subjected to damages like Hydrogen Induced Cracking (HIC) and Sulfide Stress Cracking (SSC). In this study, Acoustic Emission (AE) technique is used to monitor the cracking of steels immersed in sour media. The aim is to establish a methodology for HIC and SSC detection by AE and therefore to get more detailed information on the cracking mechanisms in steels during standard tests. The main focus of this article is the preliminary identification of the different AE sources involved during the tests performed in sour media. The methodology of identification of the different AE signals and the monitoring of HIC and SSC tests performed on different steel grades are described. The results indicate that AE can provide an early detection of cracking (HIC and SSC) when the various AE sources are identified.

Introduction

Wet hydrogen sulfide cracking of steels is a process involving Hydrogen Embrittlement (HE) in a broad range of service applications of the petroleum industry including oil and gas production, refining and gas processing. Several kinds of damage may be caused by wet H_2S in contact with low alloyed steels [1].

In low strength plates and line pipe steels, the main cracking process is Hydrogen Induced Cracking (HIC). HIC is caused by diffusion and segregation of hydrogen at internal traps, such as non-metallic inclusions, regions of anomalous microstructures (e.g., ferrite/pearlite interfaces) produced by segregation of impurities and alloying elements, and other weak interfaces. When the concentration of hydrogen at the defects reaches saturation, recombination to gaseous hydrogen occurs, with a high pressure build-up of hydrogen leading to internal cracking.

Significantly different, Sulfide Stress Cracking (SSC) leads to the failure of the metal due to the combined effect of both corrosion (resulting in hydrogen absorption) and tensile stress (residual and/or applied) in wet H_2S environment. High strength metallic materials and hard welded zones are prone to SSC. Crack initiation of SSC is always located at the surface of the metal.

Both kinds of H_2S cracking modes (HIC and SSC) of steels are studied through standard tests, respectively, NACE TM 0284-96 [2], and EFC 16 [3] or NACE TM 0177-96 [4], in sour media. These standard tests are a good tool for sour service material selection or qualification, but give no information either on kinetics or cracking mechanisms.

On the other hand, the Acoustic Emission (AE) technique is a non-destructive evaluation method ensuring the detection of active defects in materials. The associated events give rise to elastic waves which propagate within the material and result in detectable AE signals. Among the variety of mechanisms of deformation and damage that can be AE sources, corrosion processes take a particular place, as the acoustic source is often not the electrochemical corrosion driving force itself, but its consequence: bubbles

V. Smanio · J. Kittel · F. Ropital
IFP, BP3-69360 Solaize, France

V. Smanio · T. Cassagne
TOTAL, ave Larribau, 64018 Pau cedex, France

M. Fregonese (✉) · B. Normand
Université de Lyon, INSA-Lyon, MATEIS CNRS UMR 5510,
21 ave J. Capelle, 69621 Villeurbanne, France
e-mail: marion.fregonese@insa-lyon.fr

evolution, cracks propagation, growth, and evolution of corrosion products deposits, etc. [5, 6], whether corrosion is localized or uniform. Indeed, good correlations were obtained between specific AE parameters and amplitude of corrosion damage in various cases: stress corrosion cracking [5–8], abrasion or erosion corrosion [9], pitting corrosion [10–13], crevice corrosion [14, 15], exfoliation corrosion [16], uniform "acidic" corrosion [17].

Acoustic Emission technique was already applied to monitor HE in several studies [18–23]. Cayard and Kane [20] and also Gingell and Garat [22] showed that during SSC tests leading to the failure of the tested metal, a higher AE energy build-up rate was recorded compared to no-failure tests. This critical energy build-up rate associated to SSC failure remains dependant on the tested steels and on the applied stress level. Weng and Chen [19] found a correlation between HIC damage evaluated by Crack Length Ratio and the AE energy level. Moreover, Gingell and Garat [22] showed that AE could be used to discriminate initiation and propagation stages of SOHIC (Stress Oriented Hydrogen Induced Cracking) development during NACE TM0177-96 method A tensile tests [4].

Yet, in all these studies, AE data were considered in a global manner, i.e., considering simultaneously all the AE sources involved during the test. Now, all the active AE sources during HE of steels in sour media were not correlated to crack initiation and/or propagation. The behavior of steel immersed in an acidic media can be described by the following corrosion reactions [24]:

Iron anodic dissolution:

$$Fe \rightarrow Fe^{2+} + 2e^{-} \quad (1)$$

Proton reduction and gaseous H_2 bubbling at the metal surface:

$$2H^{+} + 2e^{-} \rightarrow \varepsilon H_2 \quad (2)$$

Proton reduction and absorption in the metal:

$$2H^{+} + 2e^{-} \rightarrow 2(1-\varepsilon)H_{ads} \quad (3)$$

Furthermore, in the presence of H_2S, an iron sulfide (FeS) layer grows on the steel surface. Hydrogen uptake into the material (reaction 3) is also enhanced by the presence of H_2S. In summary, potential AE sources in steels exposed to wet sour media are HE cracks initiation and/or propagation, gaseous hydrogen bubbling at the metal surface, hydrogen entry in the metal, and FeS layer evolution process.

In that context, the objective of this work was to discriminate the different involved AE sources in order to allow an early detection of both HIC and SSC development within steels, but also to monitor the different physical phenomena occurring during the test (electrochemical processes, sulfide layer evolution, crack development).

Experimental procedure

Materials

Three different steels were studied: two of them were low alloy steel plates devoted to line pipe applications and the last one was a well tubing material. One grade was Sweet Service (SwS) and two grades were Sour Service (SS), mainly due to their respective microstructure, as demonstrated below.

The chemical compositions of all steels were analyzed by optical emission spectroscopy (OES), except for carbon and sulfur, analyzed by combustion (LECO method) (Table 1).

Both line pipe steels (API X65) exhibited a low carbon content (<0.1%) compared to the C110 casing steel, which had higher mechanical properties (Table 2). The C110 grade also contained alloying elements, such as chromium and molybdenum, providing a better resistance to HE.

The tensile properties of the steels in the longitudinal direction are given in Table 2.

The microstructure of each steel was observed in the long transverse direction (LT) using an optical microscope, and after polishing down to 0.05 μm diamond suspension and etching with a Nital solution (2%vol. nitric acid and

Table 2 Mechanical tensile properties of studied steels

Steel	YS (MPa)	UTS (MPa)	El%
X65 SwS	523	649	24
X65 SS	529	571	47
C110 SS	798	887	20

YS Yield strength, *UTS* Ultimate Tensile Strength, *El* Elongation

Table 1 Chemical composition (wt%) of steels

Steel	C	Mn	Si	P	S	Cr	Ni	Mo	Cu	Nb
X65 (SwS)	0.09	1.56	0.28	0.014	0.001	0.05	0.03	0.01	0.02	0.040
X65 (SS)	0.046	1.36	0.322	0.008	0.001	0.041	0.036	0.008	0.047	0.045
C110 (SS)	0.309	0.394	0.343	0.015	0.002	0.964	0.037	0.834	0.018	0.033

ethanol). The different microstructures at the mid wall location are presented in Figs. 1 to 3.

X65 SwS and X65 SS exhibit a ferrite/pearlite microstructure. Microstructure of X65 SwS is highly oriented in the rolling direction, which can affect its HIC resistance (Fig. 1). Pearlite bands in X65 SwS are located on parallel planes at different width.

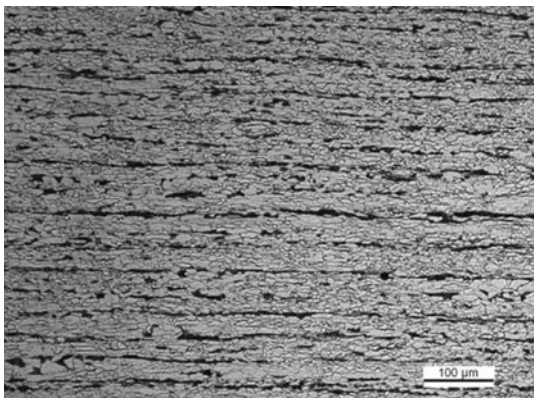

Fig. 1 Microstructure of X65 SwS grade (LT plane)

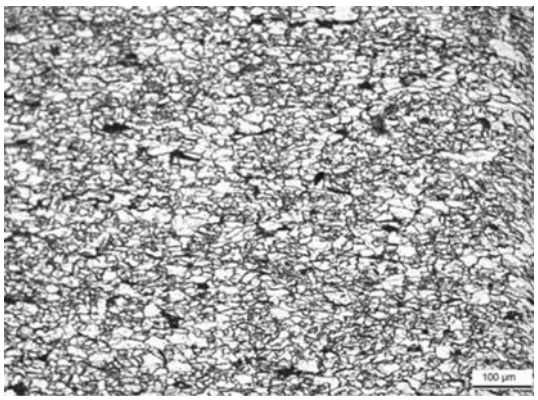

Fig. 2 Microstructure of X65 SS grade (LT plane)

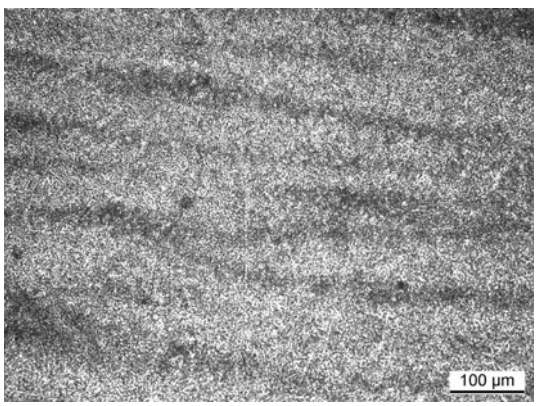

Fig. 3 Microstructure of C110 SS grade (LT plane)

For the X65 SS grade, the microstructure is equiaxed and homogenous, which accounts for its good HIC resistance (Fig. 2).

The microstructure of C110 grade is a tempered martensite with macrosegregation (Fig. 3). This microstructure is usually resistant to HIC [24].

Experimental set up

The experimental set up (Fig. 4) was based on the standard tensile test described in NACE TM0177-96 (method A) [4]. All (HIC and SSC) tests were conducted with the same experimental set up. For HIC tests, no load was applied to the test specimens. For SSC tests, a constant load was applied with the proof ring. Cylindrical tensile specimens were used for both study (HIC and SSC). Only the gauge section of the specimen was immersed in the corrosive solution. Tests were conducted in buffered solution prepared according to EFC 16 [3] (5 wt% NaCl and 0.4% CH_3COONa in distilled water) and under 1 bar H_2S. De-aeration of the solution was made by nitrogen bubbling ensuring less than 15 ppb dissolved oxygen before H_2S introduction.

A circulation of the corrosive fluid (sour media) was set-up between the test cell and a vessel, in which gas bubbling was maintained. This procedure allowed to avoid any interfering AE noise detection (e.g., gas bubbling in the test cell would result in AE) and to maintain constant electrochemical conditions in the cell during the test (easier pH control). The pH was measured with a pH meter located in this second vessel and adjusted every day with HCl or NaOH additions.

AE monitoring was performed with two AE sensors placed at the top and bottom of the specimen (Fig. 4).

AE instrumentation consisted of a transducer, a preamplifier and an acquisition device (MISTRAS with AEWIN software from Physical Acoustic Corp.). The waveforms, the events number, and the characteristic acoustic parameters were stored on a hard disk as soon as detected, and were available for treatment. For each detected AE signal, following acoustic parameters were studied:

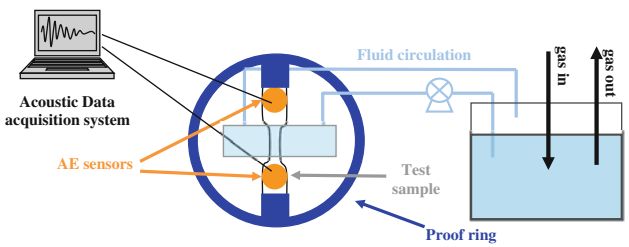

Fig. 4 Experimental set up

- Events number: number of AE signals detected (discontinuous emission),
- Amplitude: maximal amplitude of the considered AE event (peak),
- Duration: time between the first and the last overshoot of the define threshold,
- Average frequency,
- Energy: envelop of the signal.

The threshold was set to avoid recording background noise.

AE signals can be localized on the gauge length of the specimens by the use of two sensors and the measurements of the difference in the arrival time on each sensor.

Methodology

The main objective of this study was to identify the different acoustic emission sources involved when a steel sample is placed in acidic media containing H_2S.

Under these conditions, the potential physical phenomena leading to acoustic emission are:

- Electrochemical processes resulting from corrosion reactions: H_2 evolution, adsorption, proton entrance within the metal that are gathered under the terminology "H_2 evolution" in the present work,
- Formation and/or evolution of a sulfide layer on the sample,
- Cracking resulting from the absorption, the diffusion and the trapping of hydrogen, with or without applied load (HIC and SSC may proceed by different mechanisms).

Then, by varying experimental conditions and tested steels, it was possible to discriminate the different acoustic emission sources (Table 3).

A first tests batch was conducted on X65 SS steel in the presence of H_2S under cathodic polarization, with a constant current density of -0.2 mA/cm^2. For this cracking resistant steel, under cathodic polarization, the only expected AE signals should result from 'H_2 evolution'.

A second tests batch was conducted at 1 bar H_2S and pH 4.5 on the same steel (sour grade), with an applied anodic polarization (0.2 mA/cm^2). Under anodic polarization, metal dissolution and FeS layer build-up should be enhanced, while H_2 evolution and cracking are avoided. These experiments were designed to discriminate FeS layer-induced AE signals.

Then, the influence of the presence of a FeS layer at the surface of the specimen on AE signals associated to 'H_2 evolution' was studied. For that purpose, X65 SS specimens were first immersed in the solution with N_2 bubbling. Then, H_2S gas was introduced during 20 h, allowing FeS layer to form. Indeed, in these conditions the formation of a dense FeS film should be observed during about the first 8 h of test, whereas an outer porous sulfide layer should form after 24 h [21]. The third step of this procedure consisted in the application of a cathodic current (-0.2 mA/cm^2) during 3 h resulting in 'H_2 evolution' at or through the FeS layer. AE was recorded during this last step.

Once the AE characteristics of all "secondary processes" were clearly identified, AE analysis was focused on the cracking phenomenon.

Discrimination of AE signals associated to HIC was performed on X65 SwS steel tested without any polarization or any applied mechanical load at pH 4.5 in sour media. Results were compared to the ones obtained in the same experimental conditions on X65 SS steel.

Finally, C110 steel was tested at pH 3.5 under constant mechanical load (90%YS) in the presence of H_2S (1 bar) in order to discriminate AE signals associated to SSC.

After the tests, evaluation of HIC damage was performed according to the standard NACE TM0284-03 practice [2], with four equidistant cuts along the length and metallographic examination of the faces. Crack Length Ratio (CLR) and Crack Surface Ratio (CSR) were then calculated [2].

Results and discussion

AE related to H_2 evolution on bare metal

The first tests batch consisted in a cathodic polarization of the X65 SS grade immersed in the EFC 16 [3] Solution A

Table 3 Active Acoustic Emission sources as a function of experimental conditions and tested materials

Experimental conditions					Acoustic emission sources			
Gas	pH	Steel	Polarization	Load	'H_2 evolution'	Sulfide layer	HIC	SSC
N_2	4.5	X65 SS	Cathodic	No	X	–	–	–
H_2S	4.5	X65 SS	Anodic	No	Limited	X	–	–
H_2S	4.5	X65 SS	Cathodic (after FeS formation)	No	X	Limited	–	–
H_2S	4.5	X65 SS	No	No	X	X	–	
H_2S	4.5	X65 SwS	No	No	X	X	X	–
H_2S	3.5	C110	No	90%YS	X	X	–	X

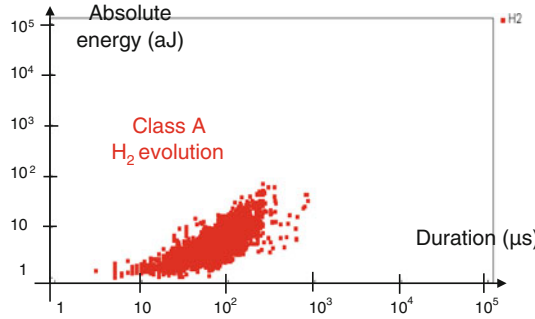

Fig. 5 Correlation chart representing absolute energy as a function of signals duration for a test conducted in the EFC 16 solution at pH 4.5 and 1 bar N_2, on a cathodically polarized X65 SS specimen

under 1 bar N_2 at pH 4.5. The applied polarization current was -0.2 mA/cm^2 and the tests lasted 8 h. The resulting potential of the sample was -100 mV/E_{corr} (-750 mV/Ag–AgCl). Cathodic reaction leading to H_2 evolution is therefore enhanced by applying a cathodic potential to the sample; at the same time, anodic reaction resulting in iron dissolution and in FeS precipitation is limited. Moreover, it was checked that no HIC does initiate under these experimental conditions.

Consequently, under these conditions, only AE sources associated with electrochemical reduction processes (hydrogen gas evolution, adsorption, proton penetration within the metal) are active. Corresponding AE results are presented in a correlation chart representing the absolute energy of the signals as a function of their duration (Fig. 5). In this figure each point represents one AE event. AE related to H_2 evolution (class A signals) exhibits the following characteristics:

- signal duration <1500 µS,
- signal absolute energy <100 aJ.

Furthermore, the average frequency of AE signals associated with 'H_2 evolution' on bare metal ranges between 0 and 250 kHz (Fig. 6) and is centered on 110 kHz.

AE related to the FeS layer

In order to identify the AE signals related to the formation and the evolution of the FeS layer on the specimen surface, further tests were performed on X65 SS at pH 4.5 under 1 bar H_2S with an anodic polarization. The resulting potential of the sample was $+70$ mV/E_{corr}. In these experimental conditions, no HIC occurs.

The characteristics of the AE signals are presented in Fig. 7. Signals associated with 'H_2 evolution' and FeS growth exhibit similar characteristics: low duration, low absolute energy. Yet, AE associated with the formation and growth of the FeS layer can be distinguished from H_2

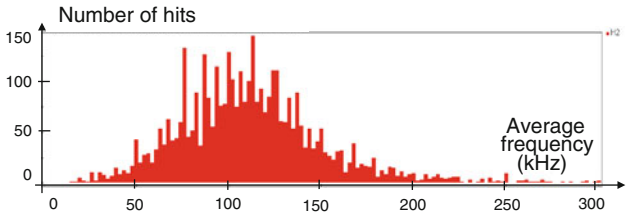

Fig. 6 Average frequency distribution of hits detected during a test conducted in the EFC 16 solution at pH 4.5 and 1 bar N_2, on a cathodically polarized X65 SS specimen

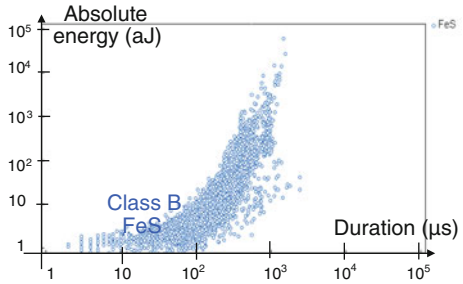

Fig. 7 Correlation chart representing absolute energy as a function of signals duration for a test conducted in the EFC 16 solution at pH 4.5 and 1 bar H_2S, on an anodically polarized X65 SS specimen

evolution signals as the absolute energy of very numerous signals is higher than 100 aJ. These high energy AE signals will therefore be considered as characteristic of FeS layer for further discrimination (class B signals). This result is in agreement with literature results [19, 21].

The average frequency distribution of AE signals recorded during these tests is plotted in Fig. 8. As observed for H_2 evolution, the average frequency of the FeS layer AE signals is between 20 and 250 kHz, but the distribution is centered between 80 and 100 kHz. The amplitude of the signals is between 32 and 80 dB and 10% of these signals exhibit amplitude higher than 44 dB. These characteristics will be used as reference to discriminate AE signals associated to the presence of a FeS layer at the surface of the specimen (Table 4).

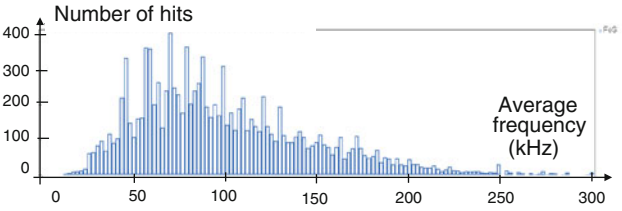

Fig. 8 Average frequency distribution of hits detected during a test conducted in the EFC 16 solution at pH 4.5 and 1 bar H_2S, on an anodically polarized X65 SS specimen

Table 4 Main characteristics of AE signals related to hydrogen evolution and sulfide layer

	Absolute energy (aJ)	Duration (μs)	Amplitude (dB)	Average frequency (kHz)
Hydrogen evolution in presence of FeS layer	<100	<1500	<44	0–200
FeS layer	10–10^5	<1500	32–80	20–250

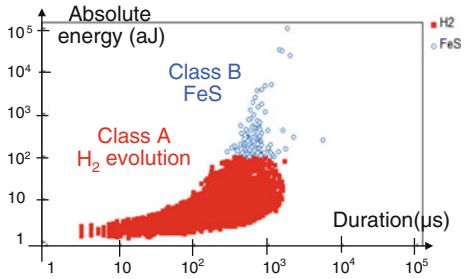

Fig. 9 Correlation chart representing absolute energy as a function of signals duration for a test conducted in the EFC 16 solution at pH 4.5 and 1 bar H_2S, on a cathodically polarized X65 SS specimen after FeS layer formation

AE related to H_2 evolution in the presence of a FeS layer on the specimen surface

Correlation chart representing absolute energy as a function of signals duration for a test conducted in the EFC 16 solution at pH 4.5 under 1 bar H_2S, on a cathodically polarized X65 SS specimen after FeS layer formation, is given on Fig. 9. It was checked again that no HIC occurs under these experimental conditions.

On this graph, some signals with absolute energies greater than 100 aJ can be detected. They can be correlated with the FeS layer, which remain an active AE source under these experimental conditions: H_2 evolution at the surface of the specimen can induce FeS layer fractures, which are active AE sources [25]. Moreover, the number of low energy (<100 aJ) but high duration (from 100 to 1500 μs) signals increases compared to previous results when H_2 evolution was occurring on a bare surface. This difference could be attributed to the presence of FeS, in agreement with literature results highlighting the higher emissivity of H_2 evolution through an oxide/hydroxide corrosion products layer at the steel surface [17].

Average frequency of the corresponding signals is ranged between 0 and 200 kHz and centered on 90 kHz (Fig. 10), as before. Therefore, the frequency distribution of H_2 evolution AE signals is not modified by the presence of a FeS layer. Amplitude of the signals is between 32 and 80 dB. Yet, 98% of the signals present amplitude lower than 44 dB.

For further HIC- and SSC-induced AE signals discrimination, these characteristics will be used for AE characterization when 'H_2 evolution' and a FeS layer occur simultaneously (Table 4) (class A + class B signals).

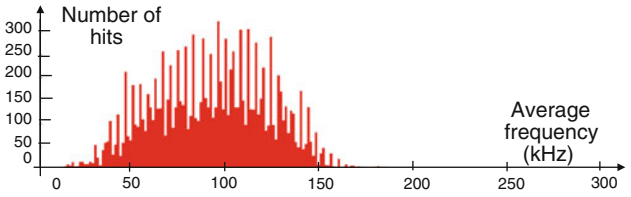

Fig. 10 Average frequency distribution of hits detected during a test conducted in the EFC 16 solution at pH 4.5 and 1 bar H_2S, on a cathodically polarized X65 SS specimen after FeS layer formation

AE related to HIC development

In order to identify the AE signals related to HIC among signals associated with H_2 evolution and an FeS layer, further tests were performed on X65 SS and X65 SwS at pH 4.5 under 1 bar H_2S. HIC assessment after these tests is given in Table 5 according to NACE TM 0284-96 Standard [2].

Cracks were only observed in the sweet service grade (X65 SwS). They were localized at the center line in the pearlite bands (Fig. 11).

AE results obtained during tests performed on X65 SS and X65 SwS steel grades are, respectively, presented in Figs. 12 and 13. As previously, H_2 evolution and FeS layer populations (respectively, class A and class B) are found, as these sources are still active in the present experimental conditions. When comparing results obtained in Fig. 13 to the previous ones, a third AE class exhibiting signals duration higher than 1500 μs is detected for X65 SwS specimen. Metallographic observations revealed the presence of cracks in the X65 SwS sample after the test. This new AE class (C) can be correlated with HIC in this steel grade.

Amplitude of class C signals is lower than 60 dB and the average frequency is between 0 and 100 kHz and centered on 40 kHz.

AE signals related to HIC development can therefore be identified as high duration and high energy but low

Table 5 HIC damage evaluation on X65 SS and X65 SwS steel grades (pH 4.5—1 bar H_2S)

	X65 SwS	X65 SS
Metallographic observations	CLR ~ 30% CSR ~ 2%	No cracks

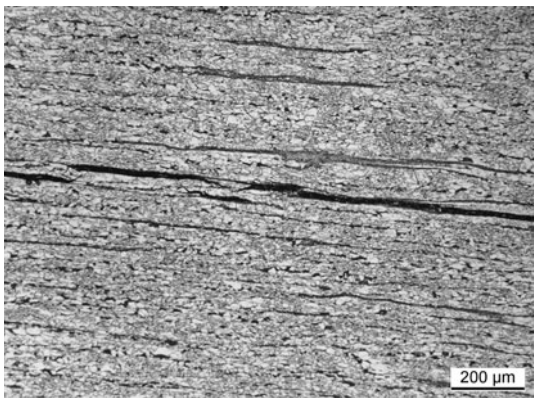

Fig. 11 HIC detected in X65 SwS after a test performed in EFC 16 solution at pH 4.5 and 1 bar H_2S

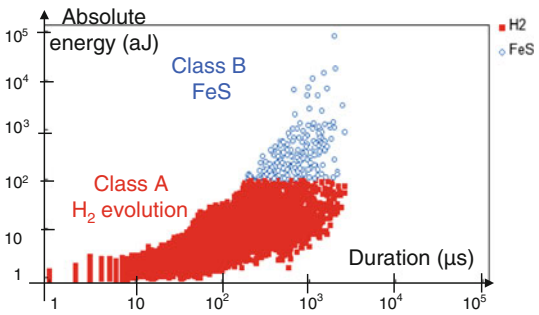

Fig. 12 Correlation chart representing absolute energy as a function of signals duration for a test conducted in the EFC 16 solution at pH 4.5 and 1 bar H_2S on a X65 SS specimen

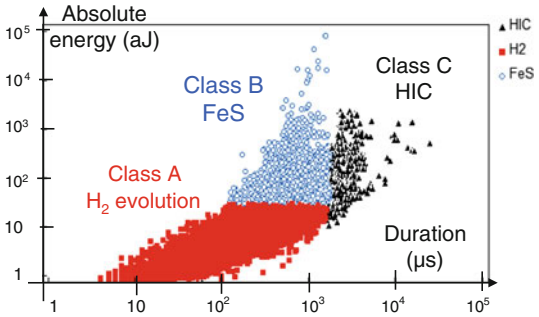

Fig. 13 Correlation chart representing absolute energy as a function of signals duration for a test conducted in the EFC 16 solution at pH 4.5 and 1 bar H_2S on a X65 SwS specimen

frequency and amplitude signals, in agreement with previous results for their energetic character [18, 19].

After identification and discrimination of the different AE signals, related to the different physical phenomena associated to HIC development within steels tested in sour media, their evolution can be monitored during the test. The cumulative energy of the three classes of AE signals was recorded during a test performed on X65 SwS steel grade at pH 4.5 under 1 bar H_2S, and is presented on Fig. 14.

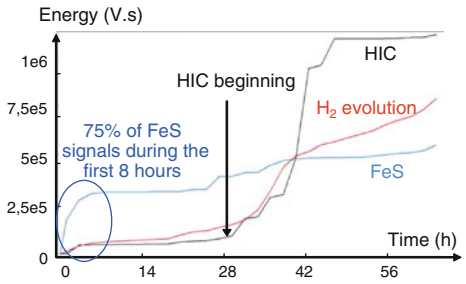

Fig. 14 Evolution of cumulative energy of the different acoustic sources during a test performed on the X65 NSS steel grade at pH 4.5 and 1 bar H_2S

During the first 8 h of the test most of the AE signals are associated with the formation of the FeS layer. This is correlated with visual observations on the specimen surface. This result is in good agreement with literature data. Tsai and Shih [21] observed that the formation of a dense FeS film lasted about 8 h in a H_2S containing solution, whereas an outer porous sulfide layer was observed after 24 h of test. The authors proposed that sulfide film formation and/or breakdown could be responsible for AE signals.

An increase of the cumulative AE energy attributed to HIC was observed after 28 h of test, which is in the same order of magnitude than the time necessary for hydrogen to diffuse and to be trapped within the material [26]. AE measurements can therefore give real time information about the incubation period required for HIC development.

Yet, it is worth noting that, even if H_2 class (class A) evolves more regularly, which is in agreement with the evolution of the physical AE source itself (electrochemical processes occur continuously), an increase of class A is also observed after 28 h of test. This increase can be due to the fact that classes A and C are certainly mixed in the junction domain of the three populations of AE signals. Further treatment of the signals would be necessary to completely discriminate the different active AE sources.

Moreover, HIC process is the physical phenomenon that induces the highest cumulative AE energy ($>1 \times 10^6$ V s). This result is in a good agreement with previous studies in which the global AE energy detected during the test was chosen as a criterion for detecting the formation of cracks [19, 20, 22].

AE related to SSC development

AE related to SSC development was studied through tests performed on C110 steel grade. Preliminary experiments confirmed that this steel grade was not susceptible to HIC (no applied stress) at pH 3.5 under 1 bar H_2S. On the other hand, when tested with a 90%YS applied load, specimens

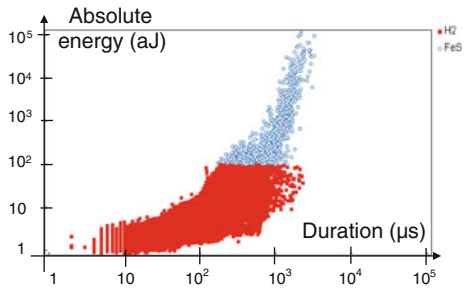

Fig. 15 Correlation chart representing absolute energy as a function of signals duration for a test conducted in the EFC 16 solution at pH 3.5 and 1 bar H_2S on a C110 specimen with an applied stress of 90% YS

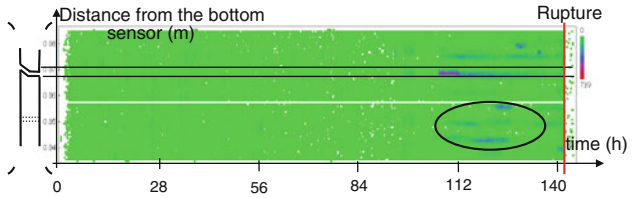

Fig. 16 Location of the density of detected AE signals on the gauge length of the specimen versus the time of test for a test conducted in the EFC 16 solution at pH 3.5 and 1 bar H_2S on a C110 specimen with an applied stress of 90% YS

failed before the end of the standard test (720 h) [4]. Time to failure ranged between 64 and 200 h.

AE results obtained during the SSC tests are displayed in Fig. 15. It is worth noting that the population of signals previously attributed to HIC (Class C—Fig. 13) is not observed. This is in agreement with the absence of detected HIC cracks within C110 grade specimens. Yet, it appears that the signals related to SSC have characteristics close to the ones of H_2 evolution (class A) and FeS layer (class B), as no additional AE signals population can be observed on the correlation chart.

Figure 16 represents the location of the density of detected AE signals on the gauge length of the specimen versus test time. Information on AE signals localization can be obtained by the calculation of the difference in arrival time of the signals on the two AE sensors coupled to the specimen (Fig. 4). The density of AE signals is quite homogeneous on the whole gauge length area, except on well defined zones where it is higher. An increase of AE signals density occurs about 40 h before the final fracture of the specimen. Several locations of high AE densities are observed on the specimen gauge length. One of the high AE signals density area corresponds to the final fracture surface, and the others are clearly correlated with the presence of short cracks on the gauge length identified by SEM (Fig. 17).

It can be concluded that AE monitoring of a standard SSC test allows to detect the early development of SSC on

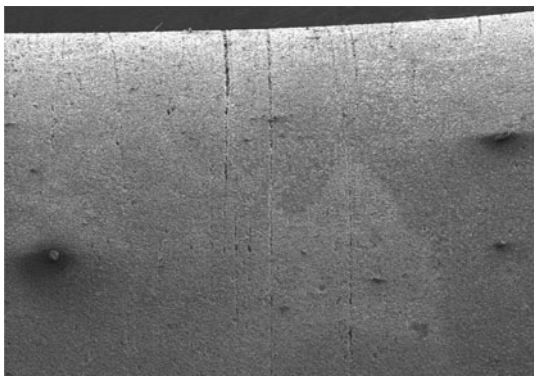

Fig. 17 SEM observation of the circle area of Fig. 16

the steel surface and to locate the initiation of cracks well before final rupture. The AE technique appears therefore to be a powerful tool to obtain real time information on initiation time and location as well as on average propagation rate during standard SSC tests. AE monitoring of SSC specimens will now be used to evaluate average crack propagation rates and to study the influence of surface parameters on SSC initiation.

Conclusions and outlook

AE monitoring was carried out during standard tests used to characterize Hydrogen Embrittlement sensitivity of steels in sour media. An experimental procedure was used to discriminate the different AE sources (H_2 evolution, FeS layer, HIC, SSC) associated with the tests. This discrimination allows settling the following conclusions:

1) AE signals discrimination was performed during HIC and SSC standard tests on several steels selected for their various susceptibility to these cracking phenomena
2) Signals associated with the three main processes have been identified
3) During HIC tests, the AE monitoring results indicate that FeS forms initially and that HIC cracks are delayed while hydrogen evolution steadily occurs during the test, as expected
4) Direct discrimination was ineffective in differentiating cracking during SSC tests. However, the increase in the localized AE signal density was clearly correlated with SSC cracks (initiated or leading to failure)
5) This work indicates that AE is a powerful technique for HIC and SSC monitoring that can give information on incubation time and cracking kinetics. This methodology will be used for the early detection of HIC in mildly sour environments and to further investigate the development of SSC. AE technique will also be

associated to hydrogen permeation measurements in order to investigate CO_2/H_2S ratio [27, 28] on SSC initiation and development.

Acknowledgements The authors would like to thank M. Boinet (Euro-Physical Acoustics), for his help in the analysis of AE data, and G. Parrain for his technical support. H. Marchebois (Vallourec) is also acknowledged for helpful discussions on H_2S cracking mechanisms.

References

1. NACE (2003) MR0175/ISO 15156-2
2. NACE (1996) International Standard Test Method NACE TM0284-96. NACE
3. Eliassen S, Smith L, Jackman P (2002) In: Oil and gas production, 2nd edn. European Federation of Corrosion (EFC number16)
4. NACE (1996) International Standard Test Method NACE TM0177-96. NACE
5. Mazille H, Rothéa R (1994) In: Tretheway KR, Roberge PR (eds) Modelling aqueous corrosion. Kluwer Academic, Netherlands, p 103
6. Yuyama S, Kishi T, Hisamatsu Y (1983) J Acoust Emission 2(1/2):71
7. Pollock WJ, Hardie D, Holroyd NJH (1982) Brit Corros J 17(3):103
8. Gerberich WW, Jones RH, Friesel MA, Nozue N (1988) Mater Sci Eng 103:185
9. Ferrer F, Idrissi H, Mazille H, Fleischmann P, Labeeuw P (1999) Wear 231:108
10. Jones RH, Friesel MA (1992) Corrosion 48(9):751
11. Mazille H, Rothea R, Tronel C (1995) Corros Sci 37(9):1365
12. Fregonese M, Idrissi H, Mazille H, Renaud L, Cetre Y (2001) J Mater Sci 36:557. doi:10.1023/A:1004891514836
13. Fregonese M, Idrissi H, Mazille H, Renaud L, Cetre Y (2001) Corros Sci 43(4):627
14. Kim YP, Fregonese M, Mazille H, Féron D, Santarini G (2003) NDT&E Int 36:553
15. Kim YP, Fregonese M, Mazille H, Féron D, Santarini G (2006) Corros Sci 48(12):3945
16. Bellanger F, Mazille H, Idrissi H (2002) NDT&E Int 35:385
17. Jaubert L, Fregonese M, Caron D, Ferrer F, Franck C, Gravy E, Labeeuw P, Mazille H, Renaud L (2005) Insight 47(8):465
18. Weng C-C, Chen R-T (1993) J Chinese Inst Eng 16(4):489
19. Weng C-C, Chen R-T (1993) J Chinese Inst Eng 16(2):195
20. Cayard MS, Kane RD (1997) Evaluation of various methods of reducing the duration of SSC qualification testing. NACE International, Paper no. 57
21. Tsai SY, Shih HC (1998) J Electrochem Soc 145(6):1968
22. Gingell ADB, Garat X (1999) Observations of damage modes as a function of microstructure during NACE TM0177-96 tensile testing of API 5L grade X60 linepipe steel. NACE International, Paper no. 600
23. Amami S, Marchand P, Duval S, Longaygue X, Fregonese M, Mazille H, Millet JP (2003) Early detection and monitoring of sulfide stress cracking (SSC) of steels by an acoustic emission method. Environmental Degradation of Engineering Materials, Bordeaux, France
24. Galland J, Sojka J, Jerome M (2004) In: Normand B, Pebere N, Richard C, Wery M (eds) Prévention et lutte contre la corrosion. Presses polytechniques et Universitaires Romandes, Lausanne, pp 273–309
25. Rawlings RD (1987) In: Kuhn AT (ed) Techniques in electrochemistry, corrosion and metal finishing. A handbook. Wiley, Brisbane, p 351
26. Kittel J, Smanio V, Fregonese M, Garnier L, Lefebvre X (2010) Corros Sci 52(4):1386
27. Liu ZY, Dong CF, Li XG, Zhi Q, Cheng YF (2009) J Mater Sci 44(16):4228. doi:10.1007/s10853-009-3520-x
28. Abelev E, Sellberg J, Ramanarayanan TA, Bernasek SL (2009) J Mater Sci 44:6167. doi:10.1007/s10853-009-3854-4